10th ANKARA INTERNATIONAL AEROSPACE CONFERENCE **AIAC-2019-049**
18-20 September 2019 - METU, Ankara TURKEY

COMPARISON OF FULLY COUPLED AND DECOUPLED MODELING RESULTS OF GRAPHITE ABLATION IN HYPERSONIC FLOWS

Oğuz Kaan ONAY[1]
ROKETSAN
Ankara, Turkey

Sinan EYİ[2]
Middle East Technical University
Ankara, Turkey

ABSTRACT

A thermochemical ablation modeling tool is developed for graphite material in air for reactive hypersonic flows. Multi-species and axisymmetric Navier-Stokes equations are solved for the flow field analysis. Arrhennius type of relations are utilized for finite rate reactions and chemical equilibrium is assumed on the eroding wall of graphite material. Total of thirteen species are included in the analysis in which eight of them are the products of the graphitic material ablation. Flow field, surface thermochemistry and axisymmetric solid conduction analysis models are fully coupled using the energy and mass balance boundary conditions on the reactive wall. Results are compared using the decoupled computational analysis and experimental data in the literature. The comparisons indicate that the coupled analysis approach provides more accurate prediction of ablation rate and wall temperature distributions. However, decoupled method is more practical to implement and provides reasonable accuracy with less computational time.

INTRODUCTION

Ablation modeling of thermal protection systems under hypersonic conditions is a critical issue in terms of the aerodynamic and thermal performance predictions of the hypersonic vehicles. Loss of the ablating material from the surface changes the species concentrations as well as thermal and transport properties inside the boundary layer. Besides, ablation products act as coolants on the surface of the vehicles. Thus, inclusion of the effect of this phenomenon is inevitable in order to evaluate the flow field around the vehicle using Computational Fluid Dynamics (CFD) analysis.

A multi-species, reacting and axisymmetric Navier-Stokes solver is developed for flow modeling. Harten-Lax-van Leer (HLL) [van Leer; Harten and Lax, 1983] flux calculation method is used for inviscid fluxes. NASA Glenn [Gordon and McBride, 1994] coefficients are utilized for thermodynamic properties of the gas mixture. Arrhenius type of finite rate reactions are used. Reaction source terms are included to the species continuity equations. Modified Wilke rule [Bird; Stewart and Lighfoot, 2002] is implemented for the calculation of mixture viscosity.

[1] Engineer, ROKETSAN - PhD Candidate, Middle East Technical University: kaan.onay@roketsan.com.tr
[2] Associate Professor, Middle East Technical University : seyi@metu.edu.tr

Diffusion terms are calculated using The Fick's law with an assumption that Lewis number is unity for laminar diffusion coefficient.

Chemical equilibrium is assumed on the eroding surface. The equilibrium coefficients of nitridation, oxidation, combination/decomposition and sublimation reactions are evaluated using empirical coefficients [Palmer and Shalef, 1965], [Baker, 1977]. Equilibrium system is coupled with flow field and conduction analyses and ablation boundary conditions. Although the usage of readily prepared lookup tables for surface species is a common approach in ablation analyses [Milos and Rasky, 1994], in this study, lookup tables are avoided in order to eliminate interpolation errors during the coupled analysis.

Initially, it is assumed that flow field is not affected from the ablation phenomena and the boundary layer edge properties are used as the boundary condition of decoupled ablation analysis. Heat transfer coefficient approximation [Zoby; Moss and Sutton, 1980] with blowing correction is used for the wall heating calculations.

After obtaining decoupled analysis results, the aerothermodynamics flow field modeling tool is fully coupled with the surface thermochemistry and conduction models and the effect of the ablation is included in the CFD calculations. Results for wall temperature, surface mass blowing rate and wall species concentration distributions are compared and discussed.

In this study, a slender sphere-cone nose geometry is selected for the numerical calculations. Ablation rate and temperature measurements of the geometry are adapted from arc-jet test results of NASA Ames Research Center [Chen; Milos and Reda, 2003]. Validation of equilibrium and finite rate modeling studies of Milos and Chen [Milos and Chen, 2005] are carried on using this test case. Besides, Bianchi et al [Bianchi; Nasuti and Martelli, 2010] have used the similar test case for comparison of their numerical calculations.

AEROTHERMODYNAMICS ANALYSIS

Axisymmetric and multispecies Navier-Stokes equations are solved in conservative variable form. A finite volume approach is used and explicit local time stepping is implemented for the convergence of solution. The flow equations for reactive flow in an axisymmetric domain are given below.

$$\frac{\partial F(W)}{\partial z}+\frac{\partial G(W)}{\partial r}-\frac{\partial F_v(W)}{\partial z}-\frac{\partial G_v(W)}{\partial r}+H+H_v-S=0 \tag{1}$$

Conservative variable vector and inviscid flux vectors in axial and radial directions are given in equation (2) respectively. Godunov type flux calculation method HLL is used for inviscid fluxes.

$$W=\begin{bmatrix}\rho\\ \rho u\\ \rho v\\ \rho e_t\\ \rho_1\\ \vdots\\ \rho_{k-1}\end{bmatrix} \qquad F=\begin{bmatrix}\rho u\\ \rho uu+p\\ \rho uv\\ (\rho e_t+p)u\\ \rho_1 u\\ \vdots\\ \rho_{k-1}u\end{bmatrix} \qquad G=\begin{bmatrix}\rho v\\ \rho uv\\ \rho vv+p\\ (\rho e_t+p)v\\ \rho_1 v\\ \vdots\\ \rho_{k-1}v\end{bmatrix} \tag{2}$$

Viscous flux vectors are shown in equation (3). All the derivatives required for the calculation of viscous terms are evaluated using grid transformation metrics. Diffusion terms are also included in the species continuity equations since these terms have an important role on the ablation phenomenon. Diffusion is the only source of reactants of nitridation and oxidation at

high temperatures near the wall. Thus, accurate prediction of diffusion fluxes is critical especially for a fully coupled solution.

$$\hat{F}_v = \begin{bmatrix} 0 \\ \tau_{zz} \\ \tau_{zr} \\ \tau_{zz}u + \tau_{zr}v + q_z + \sum J_{z,i}h_i \\ J_{z,1} \\ \cdot \\ \cdot \\ J_{z,N-1} \end{bmatrix} \quad \hat{G}_v = \begin{bmatrix} 0 \\ \tau_{zr} \\ \tau_{rr} \\ \tau_{zr}u + \tau_{rr}v + q_r + \sum J_{r,i}h_i \\ J_{r,1} \\ \cdot \\ \cdot \\ J_{r,N-1} \end{bmatrix} \tag{3}$$

Viscosity of single species is calculated using force constants as below [Svehla, 1966].

$$\mu_k = \frac{26.693\sqrt{M_{wk}T}}{{\sigma_k}^2\Omega^{(2,2)*}}x10^{-7} \tag{4}$$

Viscosity of the gas mixture is obtained using modified Wilke rule [Bird; Stewart and Lighfoot, 2003].

$$\mu = \sum_{k=1}^{ngas} \frac{X_k\mu_k}{\sum_{j=1}^{ngas} X_j\phi_{jk}} \tag{5}$$

$$\phi_{jk} = \frac{1}{\sqrt{8}}\left(1+\frac{M_{wk}}{M_{wj}}\right)^{-0.5}\left(1+\left(\frac{\mu_k}{\mu_j}\right)^{0.5}\left(\frac{M_{wj}}{M_{wk}}\right)^{0.25}\right)^2 \tag{6}$$

Laminar diffusion coefficient is calculated as shown below:

$$D = \frac{Lek}{\rho C_p} \tag{7}$$

In air, the decompositions of O_2 and N_2 molecules are expected to occur above 2000 and 4000 K, respectively. Although, ionization begins at about 9000 K, this effect is neglected in the present CFD analyses. The current finite rate reaction analysis of hypersonic flows has total of 17 steps including the third body effects and these steps are as listed below [Gardiner and Burcat, 1984].

$$\begin{gathered} O_2 + M \Leftrightarrow 2O + M \qquad M = N, NO, N_2, O_2, O \\ N_2 + M \Leftrightarrow 2N + M \qquad M = N, NO, N_2, O_2, O \\ NO + N \Leftrightarrow 2N + O \\ NO + M \Leftrightarrow N + O + M \qquad M = NO, N_2, O_2, O \\ N_2 + O \Leftrightarrow NO + N \\ NO + O \Leftrightarrow O_2 + N \end{gathered} \tag{8}$$

The following Arrhenius type of relation is used for the forward reaction coefficient calculations,

$$k_f = A_f T^{\beta_f} \exp\left({}^{-E_f}/_{RT}\right) \tag{9}$$

where A_f is the pre-exponential factor, β_f is the temperature exponent and E_f is the activation energy. Backward reaction coefficients are evaluated using the equilibrium constants K_r as shown below.

$$k_b = \frac{k_f}{K_r} \tag{10}$$

The equilibrium constants of reactions are obtained from the change of the Gibbs free energy. Entropy and enthalpy values of reactants and products are calculated using the NASA Glenn polynomial coefficients [Gordon and McBride, 1994].

IN-DEPTH ENERGY ANALYSIS

Axisymmetric heat conduction equation is solved using a finite volume approach inside the solid domain. Effect of shape change due to ablation is neglected and a Landau-like grid advection term is included in the equation [Landau, 1950], [Blackwell and Hogan, 1994]. Conduction equation in integral form is as given below in equation (11).

$$\int_s \dot{\boldsymbol{q}}''.d\boldsymbol{A} - \int_s \rho e \boldsymbol{v_r}.d\boldsymbol{A} + \frac{d}{dt}\int_v \rho e dV = 0 \tag{11}$$

In equation (11), $\dot{\boldsymbol{q}}''$ is the heat flux vector, $\boldsymbol{v_r}$ is the advection velocity due to ablation and $\boldsymbol{e}$ is the internal energy. The area vector on each edge of the control volumes are calculated as follows:

$$d\boldsymbol{A} = 2\pi r \begin{bmatrix} dr \\ -dz \end{bmatrix} \tag{12}$$

The heat flux vector is obtained with the relation below.

$$\dot{\boldsymbol{q}}'' = \begin{bmatrix} k_{zz} & k_{zr} \\ k_{rz} & k_{rr} \end{bmatrix} \begin{bmatrix} {}^{\partial T}/_{\partial z} \\ {}^{\partial T}/_{\partial r} \end{bmatrix} \tag{13}$$

Grid advection velocity due to ablation is set to be the recession velocity on the ablating wall and set to zero on the back wall. Inside the solid domain, grid advection velocity is assumed to be inversely proportional to the normal distance from the ablating surface.

$$v_r = \left(1 - \frac{r_j^{n+1}}{L_r - \int_t^{t+\Delta t} \dot{s}\, dt}\right)\dot{s} \tag{14}$$

ABLATION ANALYSIS METHOD

Thermochemical erosion in reactive flows is a multi-physics problem. Aerodynamic heating causes the increase of the wall temperature thus, the rates of the heterogeneous surface reactions increase. Boundary layer species diffuse to the eroding wall and feed the reactants to be consumed. On the other hand, sublimation of solid carbon takes place for relatively low boundary layer pressure and high temperature conditions. Meanwhile, heat is conducted inside the material. Radiation and re-radiation phenomena take place between the fluid surrounding and the eroding wall. The summary of an eroding wall boundary condition is shown in Figure 1.

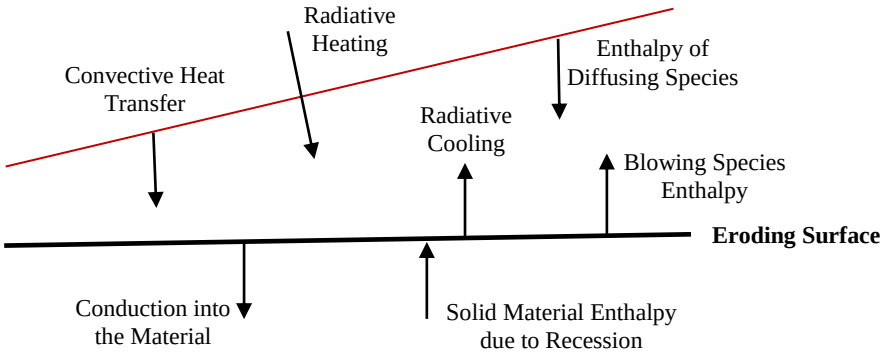

Figure 1: Summary of Thermochemical Erosion Problem

In this section, ablation boundary condition is explained for both decoupled and strongly coupled analysis methods. In the decoupled analysis, the flow field analysis results with adiabatic boundary condition are used as the boundary condition of ablation analysis. Heat transfer coefficient approximation and empirical blowing correction is implemented. On the other hand, aerothermodynamics and in-depth energy analyses are solved simultaneously via satisfying the ablation boundary condition for coupled analysis approach. Below in figure 2, flow charts of decoupled and coupled analyses are compared.

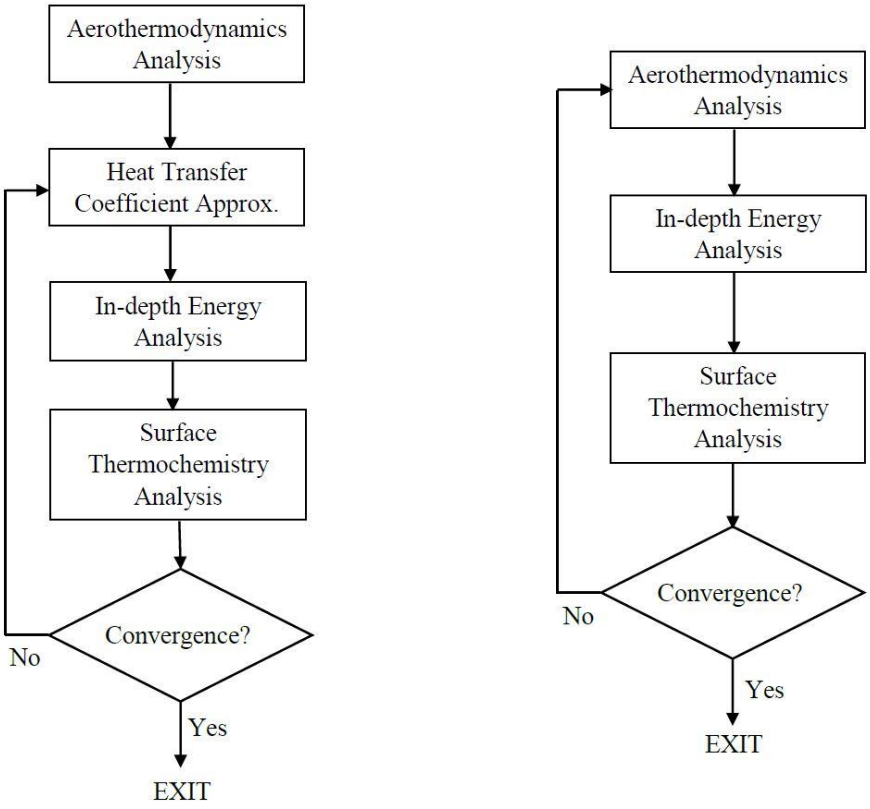

(a) (b)

Figure 2: Flowcharts of (a) decoupled analysis and (b) coupled analysis approaches

Decoupled Analysis Approach

Assuming that the boundary layer edge properties are not affected from the wall erosion products and the heat and mass transfer coefficients can be approximated, ablation boundary condition can be written as given below. The relation given is an appropriate form, where the heat and mass transfer coefficients are not equal to each other.

$$-k\frac{\partial T}{\partial \eta} = \rho_e u_e S_t (h_r - h_w)_e + \rho_e u_e S_m \sum_{i=1}^{N} (y_{ei} - y_{wi}) h_w + \dot{m}_s h_s - \dot{m}_s h_w - \sigma \varepsilon T^4 \qquad (15)$$

The left hand side of the above equation is the heat transfer to the solid domain. The terms on the right hand side are convective heating, energy transfer with mass diffusion, solid enthalpy entering the ablating surface with recession, blowing enthalpy and the radiative cooling of the solid surface respectively.

The elemental mass balance can be written as shown below if equal diffusion coefficients is assumed for the species [Bianchi, 2007]. The first term is the wall species concentration, second term is the species concentration inside the solid domain and the third term is the boundary layer edge species concentration.

$$(1 + B')y_{wi} - B'y_{ci} - y_{ei} = 0 \qquad (16)$$

Dimensionless mass blowing parameter, *B′*, is a measure of blowing rate from the ablating surface and it is defined by nondimensionalizing the mass blowing rate with the mass transfer coefficient. It is one of the most critical parameters to be obtained with the surface thermochemistry calculations especially for equilibrium surface thermochemistry assumption.

$$B' = \frac{\dot{m}}{\rho_e u_e C_m} \tag{17}$$

Unblown heat transfer coefficient should be corrected as shown below. A moderate reduction of the coefficient is expected for a blowing wall.

$$S_t = S_{t0} \frac{ln(1 + 2\lambda B')}{B'} \tag{18}$$

Energy balance equation can be reduced to a more compact form if Le=1 is assumed.

$$-k \frac{\partial T}{\partial \eta} = \rho_e u_e S_t (h_r - (1 + B')h_w) + \dot{m}_s h_s - \sigma \varepsilon T^4 \tag{19}$$

Unblown heat transfer rate for decoupled analysis is approximated using the relation below [Zoby; Moss and Sutton, 1980].

$$\dot{q}_{w,0} = Re_\theta^{-1} \left(\frac{\rho^*}{\rho}\right) \left(\frac{\mu^*}{\mu}\right) \rho_e u_e (h_{aw} - h_w) Pr_w^{-0.6} \tag{20}$$

Reference density ρ^* and reference viscosity μ^* values are calculated at reference temperature defined by Eckert [Eckert, 1961].

$$T^* = 0.5T_w + 0.22T_{aw} + 0.28T_e \tag{21}$$

Transfer coefficient can be calculated from the unblown heat transfer rate as given:

$$\rho_e u_e St_0 = \frac{\dot{q}_{w,0}}{h_r - h_w} \tag{22}$$

Recovery enthalpy term h_r in the above equation is obtained from the aerothermodynamics analysis and the wall enthalpy h_w is calculated from wall temperature value during the ablation analysis.

Fully Coupled Analysis Approach

Energy balance for strongly coupled modeling approach includes the gradient terms of species concentrations and temperature gradients adjacent to the eroding wall. The terms on the left hand side of the energy balance equation are heat conduction on fluid side, enthalpy diffusion because of species diffusion and the solid enthalpy entering to the control surface respectively. The terms in the right hand side are blowing species enthalpy, heat conduction on the solid side and radiative cooling of the wall. Gradient terms are calculated using grid transformation metrics of the wall adjacent cells of the fluid side. Unity emissivity is assumed for radiation term.

$$k_f \frac{\partial T}{\partial \eta}\bigg|_f + \sum_{i=1}^{N} h_i \rho\, D_i \frac{\partial y_i}{\partial \eta}\bigg|_f + \dot{m}_s h_s = (\rho v)_w h_w - k_s \frac{\partial T}{\partial \eta}\bigg|_s + \sigma \varepsilon T^4 \tag{23}$$

The mass balance equation for each species of the flow field including the ablation products is as given below. The first term on the left hand side of the equation is the diffusion of species to the wall, second term is the species source by the heterogeneous surface reactions and the term on the right hand side is the blowing of the species from the eroding wall.

$$\rho D_i \frac{\partial y_i}{\partial \eta}\bigg|_f + \dot{w}_i = (\rho v)_w y_i \tag{24}$$

Ablating Surface Thermochemistry

For graphite ablation in air, the following nitridation, oxidation, combination/decomposition and sublimation reactions are utilized to evaluate wall species concentrations.

$$\begin{gathered} O_2 \Leftrightarrow 2O \\ N_2 \Leftrightarrow 2N \\ CO + O \Leftrightarrow CO_2 \\ C + O \Leftrightarrow CO \\ C + N \Leftrightarrow CN \\ C(s) \Leftrightarrow C \\ 2C(s) \Leftrightarrow C_2 \\ 3C(s) \Leftrightarrow C_3 \\ 4C(s) \Leftrightarrow C_4 \\ 5C(s) \Leftrightarrow C_5 \end{gathered} \tag{25}$$

In the ten equations above, there are total of twelve chemical species. The equilibrium constant for each reaction can be written as a function of partial pressures and stoichiometric coefficients of the species.

$$K_p = p_j^{v_j} p_i^{-v_i} \tag{26}$$

In the equation above, $\boldsymbol{K_p}$ is the equilibrium constant of a reaction. $\boldsymbol{p_i}$ and $\boldsymbol{p_j}$ are the partial pressures and, $\boldsymbol{v_i}$ and $\boldsymbol{v_j}$ are the stoichiometric coefficients of the reactants and products, respectively. The equilibrium constants can be evaluated as a function of the wall temperature as follows:

$$10^{a}10^{-b/T} - p_j^{v_j} p_i^{-v_i} = 0 \tag{27}$$

The equation set of the chemical equilibrium system is solved using Newton iterations for the prediction of the wall species concentrations from partial pressure values. Solution of linearized system is performed simultaneously with the flow field and solid conduction analyses. Calculated wall species mass fractions are supplied to the energy and mass balance equations.

RESULTS AND DISCUSSIONS

An arc-jet test case of a slender nose-tip geometry with nose radius of 1.95 cm is selected from literature [Chen; Milos and Reda, 2003] for the CFD and ablation analyses. In this test case, ablating material is pure graphite and free stream conditions are as given in Table 1. Numerical grid generated for the analyses is shown in Figure 3. 108x66 and 108x30 structured cells are used for the fluid and solid domains respectively.

Table 1: Free Stream Boundary Condition for Hypersonic Flow Case – Arc-Jet Data [Chen; Milos and Reda, 2003]

T_∞	V_∞	ρ_∞	O_2	O	N_2	N	NO
1428 K	5354 m/s	0.003 kg/m^3	0.0000	0.2573	0.6169	0.1212	0.0046

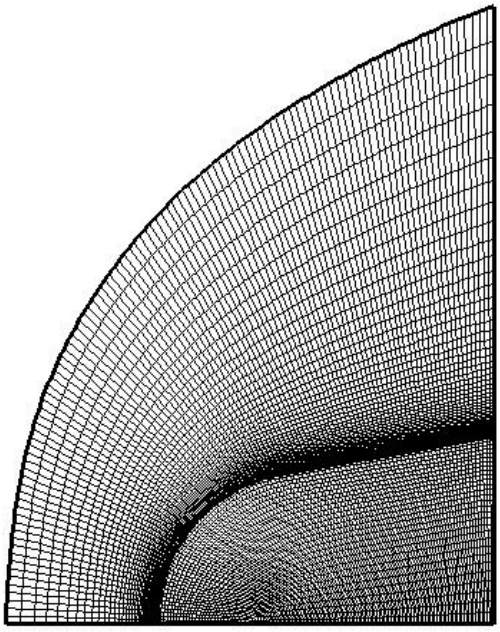

Figure 3*:* Computational Grids of Fluid and Solid Domains

Initially, flow field results are calculated with adiabatic wall boundary condition. Boundary layer edge properties of this solution are extracted and used for heat and mass transfer rate approximations in the decoupled analysis. Then, surface thermochemistry, in-depth energy and flow field analysis tools are strongly coupled and the calculations are carried on simultaneously. Energy and mass balance boundary conditions are satisfied for both fluid and solid domain calculations. The comparison of temperature contours for adiabatic and ablating wall boundary conditions are shown in Figure 4.

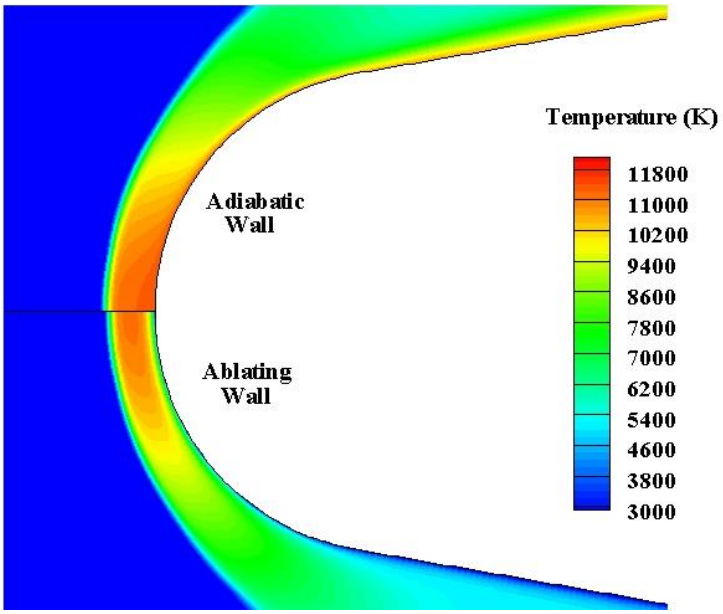

Figure 4*:* Comparison of Temperature Contours for Adiabatic and Ablating Wall Boundary Conditions

Distributions of C_3, CO, NO and N_2 mass fractions near the ablating wall are given in Figure 5 for coupled analysis. C_3 and CO are the dominant species produced by graphite ablation. C_3 is a product of sublimation and CO is a product of oxidation reaction. Near the stagnation point, wall temperature is relatively higher as expected, thus the ablation is mostly in sublimation regime. On the other hand, CO mass fraction near the ablating wall increases with increasing distance from the stagnation point. NO and N_2 mass fraction distributions are given as examples of the flow field species. Maximum NO mass fraction is observed on the intersection of stagnation line and the bow shock. Besides, decomposition of N_2 molecules can be seen with the increase of temperature behind the bow shock. Near the wall, fluid temperature decreases due to cooling effect of ablation and recombination of N atoms take place. In literature [Bianchi; Nasuti and Martelli, 2010], [Park, 2004], [Park, 2007] it is stated that the recombination of N atoms near the wall is negligible and this reaction can be considered as inactive near the wall. This reaction is not assumed to be frozen during the analysis since the effect of recombination near the wall is out of the scope of the current study.

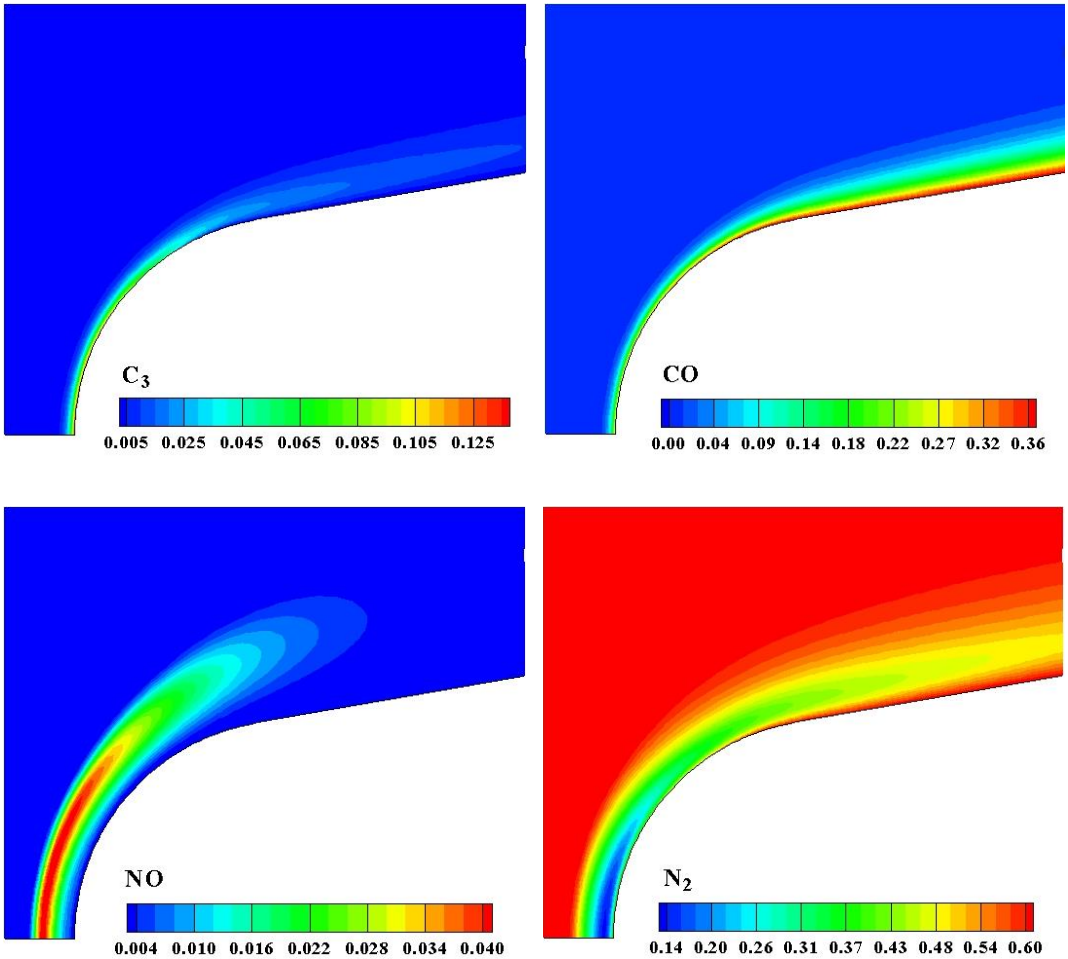

Figure 5: Mass Fraction of C_3, CO, NO and N_2 inside the Flow Field (fully coupled analysis)

Calculated mass fraction distributions of dominant ablation products on the wall are given in Figure 6. Mass fraction of C_3 is calculated relatively higher with the decoupled analysis. Higher temperature values are obtained with the heat transfer coefficient approximation, thus the sublimation rate is higher than the fully coupled approach. On the other hand, in the conjugate analysis, the mass fraction of oxidation product CO is calculated relatively higher than the decoupled analysis.

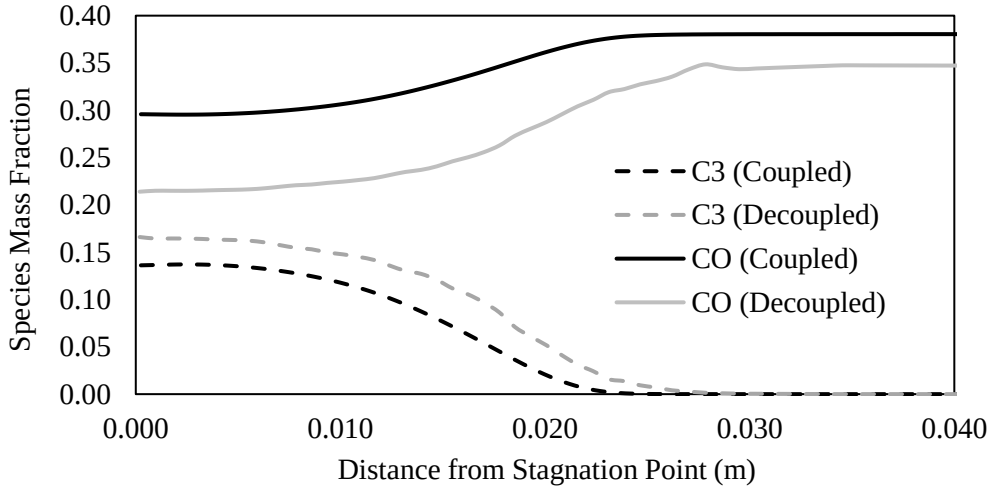

Figure 6: Mass Fraction of C_3 and CO on the Ablating Wall (Streamwise Direction)

Temperature contours inside the graphite specimen are given in Figure 7 for both coupled and decoupled analyses. Besides, comparison of calculated wall temperature distributions with experiment data are shown in Figure 8. Overestimation of temperature is observed with the decoupled approach. Relatively more accurate results can be obtained with the coupled analysis especially on the region close to the stagnation point. Error of the calculated wall temperature increases with increasing distance from the stagnation point in both of the methods. Wall equilibrium assumption of surface thermochemistry calculation begins to fail with decreasing temperature. Bianchi et al states that [Bianchi; Nasuti and Martelli, 2010] equilibrium assumption is valid up to wall temperature of ~2500 K for graphite in air ablation.

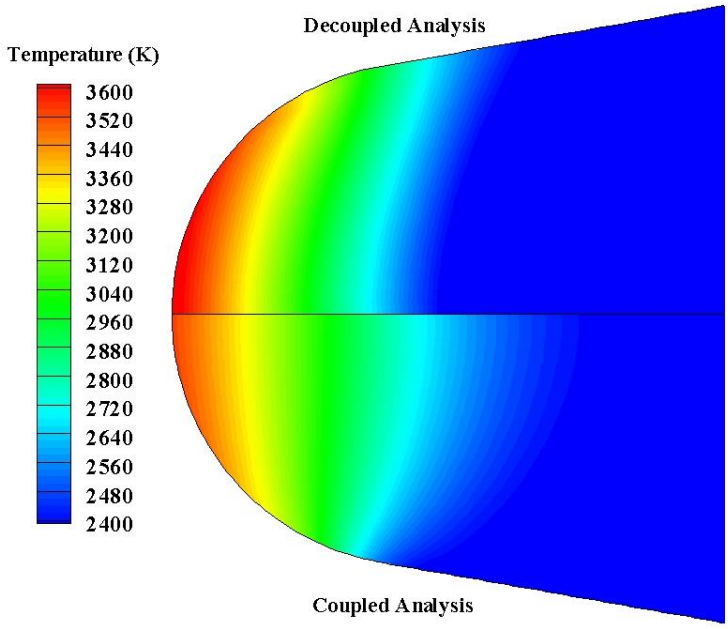

Figure 7*:* Comparison of Temperature Distributions inside the Solid Domain

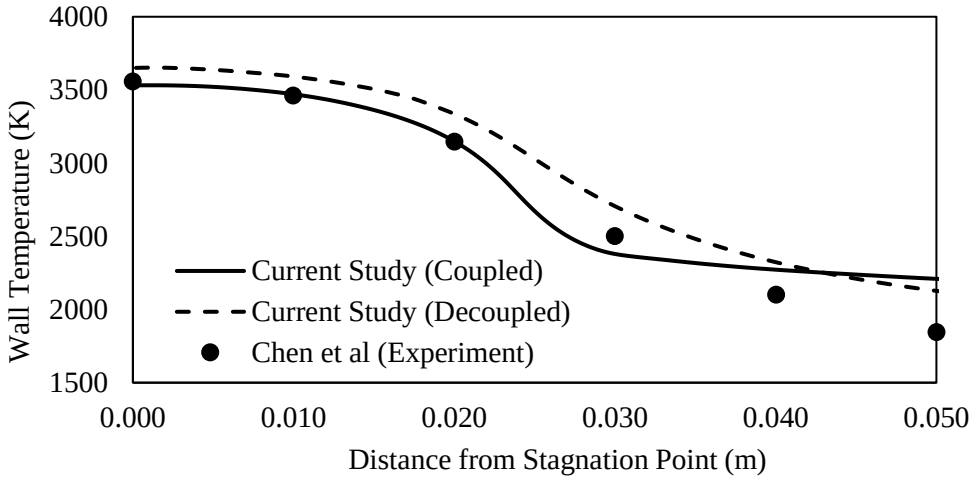

Figure 8*:* Comparison of Calculated Wall Temperature Distributions with Experiment Data [Chen; Milos and Reda, 2003]

In figure 9, calculated blowing rate distributions are compared with the experiment results [Chen; Milos and Reda, 2003] and computational results from the literature [Bianchi; Nasuti and Martelli, 2010]. In the current study, mass blowing rate is overestimated about 10% and 25% on the stagnation point using coupled and decoupled analyses respectively. On the other hand, calculated value is underestimated about 13% with the coupled analysis and overestimated about 30% with the decoupled analysis on the 45^0 point of the nose-tip.

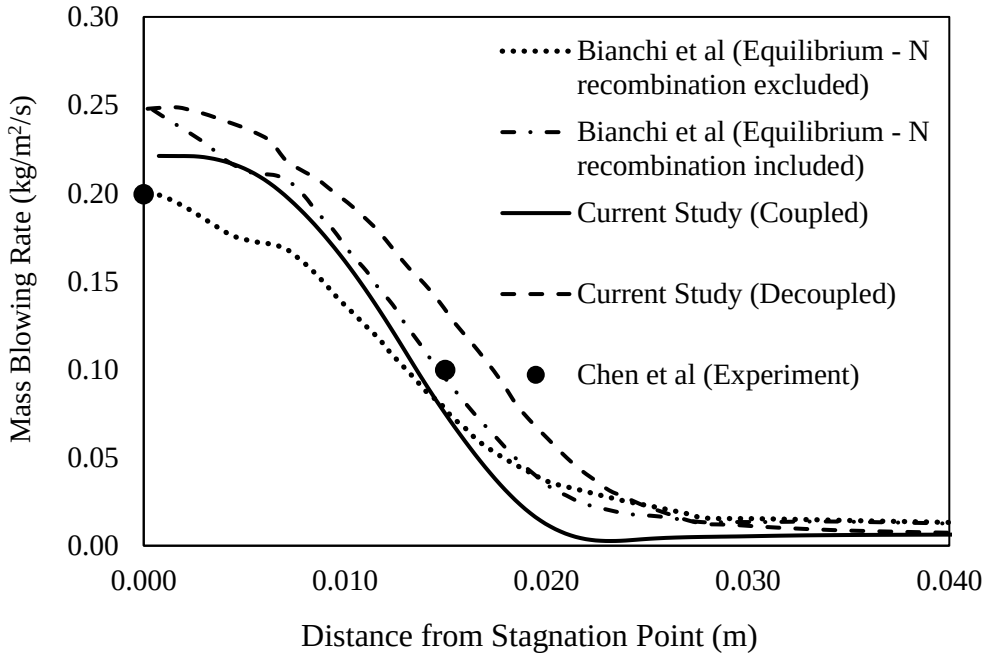

Figure 9*:* Comparison of Calculated Mass Blowing Rate with Experiment [Chen; Milos and Reda, 2003] and Literature Data [Bianchi; Nasuti and Martelli, 2010]

Although the coupled analysis has a superior accuracy, decoupled analysis is more advantageous in terms of computational cost. In the coupled analysis, flow field is resolved with adiabatic wall boundary condition initially. Then, the conjugate analysis is carried on with a decreased CFL number. The computational time of the coupled analysis is about 17 hours. On the other hand, decoupled analysis takes about 140 minutes including a flow field solution with adiabatic wall boundary condition and a separate ablation analysis.

CONCLUSION

In this study, an ablation analysis tool is developed for graphite-in-air ablation problem for reactive hypersonic conditions. Flow field results are presented for a fully coupled ablation model in order to reveal the effect of cooling in the boundary layer of the hypersonic vehicle nose. Calculated wall temperature, blowing rate and the mass fractions of the ablation products are compared for coupled and decoupled modeling approaches. Results show that, coupled analysis gives more accurate results than the decoupled analysis but, decoupled method has superiority in terms of computational time. Resolving flow field separately with an adiabatic wall boundary condition and using the boundary layer edge properties as the boundary condition of the ablation analysis is a fast implementation. This method might serve a practical analysis option during the preliminary design processes. On the other hand, heat transfer coefficient approaches are usually defined for certain flow conditions and applicable to restricted geometries. These empirical formulations are generally difficult to generalize. Conjugate analysis approach overcomes this generalization problem since the thermal

boundary layer and species gradients are resolved without a transfer coefficient approximation or an empirical blowing correction.

References

Baker, R. L. (1977), Graphite Sublimation Chemistry Nonequilibrium Effects, AIAA Journal, Vol. 15, No. 10, pp. 1391-1397, Oct 1977.

Bianchi, D. (2007), Modeling of ablation phenomena in space applications, Ph.D. Thesis, Universita degli Studi di Roma, La Sapienza, 2007.

Bianchi, D., Nasuti, F. and Martelli E. (2010), Navier–Stokes Simulations of Hypersonic Flows with Coupled Graphite Ablation, Journal of Spacecraft and Rockets, Vol. 47, No. 4, pp. 554-562, Aug 2010.

Bird, R. B., Stewart W. E. and Lighfoot, E. N. (2002), Transport Phenomena, Second edition, Wiley, pp. 26-27, 2002.

Blackwell, B. F., and Hogan R. E. (1994), One-Dimensional Ablation Using Landau Transformation and Finite Control Volume Procedure, Journal of Thermophysics and Heat Transfer, Vol. 8, No. 2, pp. 282-287, Jun 1994.

Chen, Y. K., Milos, F. S., Reda, D. C., and Stewart, D. A. (2003), Graphite Ablation and Thermal Response Simulation under Arc-Jet Flow Conditions, AIAA Paper 2003-4042, Jun 2003.

Eckert, E.R.G. (1961), Survey on Heat Transfer at High Speeds, U.S. Air Force, ARL 189, Dec 1961.

Gardiner, W. C. and Burcat, A. (1984), Combustion Chemistry, Springer-Verlag New York Inc., 1984.

Landau, H. G. (1950), Heat Conduction in a Melting Solid, Quarterly of Applied Mathematics, Vol. 8, No. 1, pp. 81-94, 1950.

McBride, B. J., Zehe, M. J. and Gordon, S. (2002), NASA Glenn Coefficients for Calculating Thermodynamic Properties of Individual Species, NASA/TP-2002-211556, Sep 2002.

Milos, F. S., and Chen, Y. K. (2005), Navier–Stokes Solutions with Finite Rate Ablation for Planetary Mission Earth Reentries, Journal of Spacecraft and Rockets, Vol. 42, No. 6, pp. 961-970, Dec 2005.

Park, C. (2004), Stagnation-Point Radiation for Apollo 4, Journal of Thermophysics and Heat Transfer, Vol. 18, No. 3, pp. 349–357, Sep 2004.

Park, C. (2007), Calculation of Stagnation-Point Heating Rates Associated with Stardust Vehicle, Journal of Spacecraft and Rockets, Vol. 44, No. 1, pp. 24–32, Feb 2007.

Scala, S. M., and Gilbert, L. M. (1965), Sublimation of Graphite at Hypersonic Speeds, AIAA Journal, Vol. 3, No. 9, pp. 1635-1644, Sep 1965.

Svehla, R. A. (1966), Estimated Viscosities and Thermal Conductivities of Gases at High Temperatures, NASA-TR-R-132, 1966.

van Leer, B., Harten, A. and Lax, P. D. (1983), On Upstream Differencing and Godunov-Type Schemes for Hyperbolic Conservation Laws, SIAM Review, Vol. 25, No. 1, pp. 35-61, Jan 1983.

Zoby, E. V., Moss, J., N., Sutton, K. (1980), Approximate Convective-Heating Equations for Hypersonic Flows, Journal of Spacecraft, Vol. 18, No. 1, pp. 64-70, Jun 1980.